Retrieval advances of BrO/SO2 molar ratios from NOVAC

This Master thesis has been carried out by Elsa Wilken

at the

Institute for Environmental Physics, University of Heidelberg,

Germany

under the supervision of

Prof. Ulrich Platt

Contents

3 Remote sensing of volcanic gases

In this thesis we are interested in the volcanic trace gases SO_2 and BrO, both measured with the Differential Optical Absorption Spectroscopy (DOAS) a remote sensing technique proposed by Platt and Stutz [2008]
This chapter will give a short overview about the measuring technique.

Beer-Lambert Law

This section will give an overview about the reasons for decreasing light intensity when going through a medium.
The Lambert Beer law describes the attenuation of light when traveling through a material.

Atoms and Molecules exists in several energy states, depending on the different electron configuration. Moreover Molecules have additionally rotation and vibration states, also enclose to the energy states. If a photon matches the energy gap between two possible energy states, this includes, that the lower energy state is occupied and the selection rules are fulfilled, the molecule could absorb the photon, remaining in a higher energy state.
The additional photon energy could be loosed by collision with another molecule or by emission. But since the direction of the emitted photon is mostly not the same direction of the absorbed photon the intensity I_0 of the light before passing the medium is higher than the intensity I after traveling the distance L through the medium.
This can be described as:

$$I(L, \lambda) = I_0(\lambda) \cdot expt\left(-\int_0^L \sigma(\lambda, p, T) \cdot c(l)\, dl\right) \tag{3.1}$$

where $c(l)$ is the location-dependent concentration of the trace gas of interest. $\sigma(\lambda, p, T)$ is the absorption cross section, $\sigma(\lambda, p, T)$ is unique for each molecule and depends on pressure p and on the temperature T.
An important quantity used in many optical remote sensing techniques is the optical density τ. The optical density is a measure for the weakening of radiation when going through a material. τ can be calculated using the lambert beer law:

$$\tau = -ln\left(\frac{I(\lambda)}{I_0(\lambda)}\right) = \sigma \cdot S \tag{3.2}$$

Hereby is S the column density. The column density is the concentration of the trace when integrating along the light path, the dimension of S is therefore the number of molecules divided by an area: $\frac{molec}{cm^2}$.

$$S = \int_0^L c(l)\,dl \tag{3.3}$$

When measuring at a volcano, that means measuring in the atmosphere the situations gets more complex, since we need to deal with several absorbers and scattering processes have to be taken into account. One possibility is to treat scattering effects as pseudo absorbers with the respective extinction coefficients for Rayleigh (ϵ_R) and Mie (ϵ_M) scattering

$$I(L,\lambda) = I_0(\lambda) \cdot expt\left(-\int_0^L \sum_j \sigma_j(\lambda,p,T) \cdot c_j(l) + \epsilon_R(\lambda,l) + \epsilon_M(\lambda,l)\,dl\right) \tag{3.4}$$

The first term of eq. (3.4) in the exponential function, multiple absorbers j are considered, the corresponding concentration depends on the position l of the light path. The last two terms in describe the extinction due to Rayleigh and Mie scattering in the atmosphere.
Inelastic scattering (for example the Ring effect) and effects due to turbulences in the atmosphere, are neglected here.

3.1 Differential Optical Absorption Spectroscopy(DOAS)

It is impossible to distinguish between various broad-band effects, like scattering in the atmosphere or instrument effects which influence the measured spectra Lübcke [2014]. Therefore eq. (3.4) cannot be applied to real measurements.
Differential Optical Absorption Spectroscopy (DOAS) was invented in the late 1970s by Perner and Platt [1979]. This section will give an overview about the DOAS technique. More detailed information ca be found in the work of Platt and Stutz [2008]

Differential Optical Absorption Spectroscopy uses the fact, that absorption can be divided into broad-band parts and narrow-band parts. Broad band parts are effects that only changes weakly with the wavelength, i.e. scattering and instruments effects have a broad-band structure. The narrow band part includes effects that strongly depends on the wavelength. Within the DOAS-Method only narrow-band absorption features of molecules are used to obtain their column densities. The absorption cross section of trace gases j have broad-band ($\sigma_b(\lambda)$) and narrow band ($\sigma'(\lambda)$) features, only the narrow-band structures are used in DOAS.

$$\sigma(\lambda) = \sigma_b(\lambda) + \sigma'(\lambda) \tag{3.5}$$

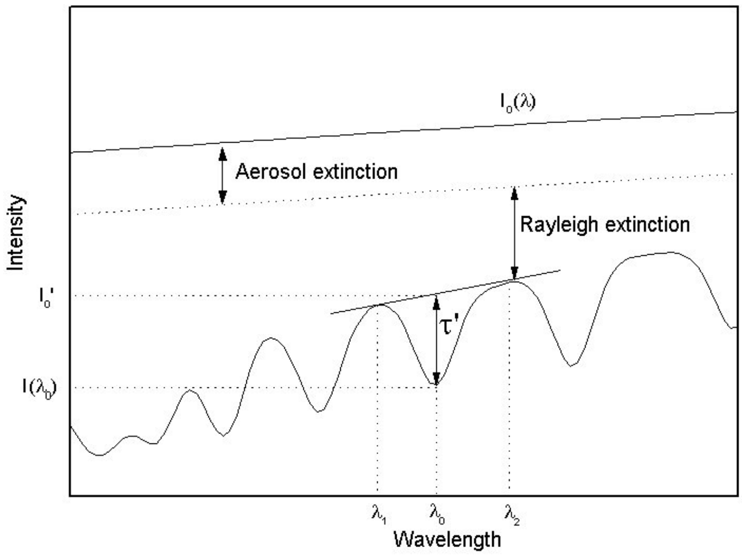

Figure 3.1: Basic idea of the DOAS principle: Light attenuate due to broad band and narrow band effects. The broad band extinction is caused by aerosols and Raylight scattering $\left(I_0 \rightarrow I'\right)$. The measured intensity I is formed by narrow band effects due to differential absorption structures by trace gases with the optical density τ'. Adapted from Kern [2009]

With this considerations the Lambert-Beer law eq. (3.4) can be rewritten dividing the exponential part into a narrow-band part and a broad-band part:

$$I\left(\lambda, L\right) = \overbrace{I_0\left(\lambda\right) \cdot exp\left(-\int_0^L \sum_j \sigma_{b,j}\left(\lambda, p, T\right) \cdot c_j\left(l\right) + \epsilon_R\left(\lambda, l\right) + \epsilon_M\left(\lambda, l\right) dl\right)}^{=I_0'(\lambda)} \cdot$$
$$exp\left(-\int_0^L \sum_j \sigma_j'\left(\lambda, p, T\right) \cdot c_j\left(l\right) dl\right) \tag{3.6}$$

The so defined $I_0'\left(\lambda\right)$ differs from $I_0\left(\lambda\right)$ only by broad band effects. With $I_0'\left(\lambda\right)$ a differential optical density τ' can be defined:

$$\tau' = ln\left(\frac{I_0'\left(\lambda\right)}{I\left(\lambda\right)}\right) = \int_0^L \sum_j \sigma_j' \cdot \left(\lambda\right) \cdot c_j\left(l\right) dl = \sum_j \sigma_j'\left(\lambda\right) \cdot S_j \tag{3.7}$$

The optical density can now be calculated by using the difference of the column density S_M in the measurement spectrum to the column density S_R of a reference spectrum. From Equation (3.6) we know:

$$I_{P,R} = I_0' \cdot exp\left(-S_{P,R} \cdot \sigma\left(\lambda\right)\right) \tag{3.8}$$

In general the obtained column density S_M is called differential slant column density: "dSCD". If the reference spectrum does not contain the trace gas of interest (is not contaminated with trace gases) that means $S_R = 0$, S_M is called the slant column density (SCD). With Equation (3.8) the optical density can be derived by:

$$\tau(\lambda) = -ln\left(\frac{I_M}{I_R}\right) = \sigma(\lambda) \cdot (S_M - S_R) \tag{3.9}$$

3.1.1 Technical Implementation of the DOAS Approach

The theory explained above only describes the ideally situation. In real measurements more problems occur due to instrument limitations inelastic scattering causing the Ring effect and due to impacts of external parameters like temperature.
In the following a short overview about these problems and their consequences for our retrieval is given. Further information can be found in Lübcke [2014].

Optical and spectral resolution of the spectrometer

The resolution of the spectrometer is finite, thus, the detector receives a spectrum $I^*(\lambda)$ which can be retrieved with a convolution of the incident spectrum $I(\lambda)$ with the instrument function H(λ):

$$I^*(\lambda) = I(\lambda) * H(\lambda) = \int I(\lambda - \lambda') \cdot H(\lambda - \lambda')\, d\lambda' \tag{3.10}$$

For the evaluation all σ_j of the trace gases of interest need to have the same spectral resolution as the instrument used for recording the spectra. In this work we will use high resolution cross sections and convolute them with the instrument function H:

$$\sigma*(\lambda) = \sigma(\lambda) * H(\lambda) \tag{3.11}$$

The instrument function H can be approximated by using a the spectral lines of an mercury lamp since the width of those lines is only a few pm, they could be treated as delta peaks when comparing it to the resolution of the spectrometers.

Effects of the detector

The detector only has discrete pixels, therefore a wavelength interval is mapped to a pixel i.

$$I^{'}(i) = \int_{\lambda(i)}^{\lambda(i+1)} I^*(\lambda' d)\, d\lambda' \tag{3.12}$$

For the retrieval the relationship between the detector channels and the wavelength of the spectrum need to be known. The wavelength to pixel mapping (WMP) for a detector with q channels can be calculated as:

$$\lambda(i) = \sum_{k=0}^{q-1} \gamma_k \cdot i^k \tag{3.13}$$

Hereby, is γ_0 a shift of the spectrum and γ_1 is a squeeze (respectively stretch) of the spectrum. The wavelength to pixel mapping can be discovered by using a mercury lamp again and compare pixel-position with the well known wavelength of the individual HG-lines of the mercury lamp.
The wavelength to pixel mapping depends on the instrument temperature as well as on the ambient pressure Lübcke et al. [2014].

Ring effect

As mentioned above inelastic scattering causes the Ring effect (named after Grainger and Ring, 1962). The Ring effect is observable through a filling of the Fraunehofer lines in spectra of scattered solar radiation, (e.g. if the sunlight travels through the earth atmosphere). When compared to direct sunlight measurements (e.g. outside of the earth atmosphere). (Bussemer [1993],Solomon et al. [1987]), proposes that the Ring effect is a result of rotational Raman scattering mainly of O_2 and N_2 in the atmosphere. Solomon et al. [1987] suggested to treat the Ring effect as a pseudo-absorber.

B Bibliography

NOVAC novac-site. http://www.novac-project.eu/. Accessed: 2018-01-29.

Python scikit-learn.org. http://scikit-learn.org/stable/modules/generated/sklearn.linear_model.LinearRegression.html. Accessed: 2018-01-19.

Nicole Bobrowski, R Von Glasow, A Aiuppa, S Inguaggiato, I Louban, OW Ibrahim, and U Platt. Reactive halogen chemistry in volcanic plumes. *Journal of Geophysical Research: Atmospheres*, 112(D6), 2007.

Markus Bussemer. Der ring-effekt: Ursachen und einfluß auf die spektroskopische messung stratosphärischer spurenstoffe. *Diplomathesis, University of Heidelberg*, 1993.

K Chance and RL Kurucz. An improved high-resolution solar reference spectrum for earth's atmosphere measurements in the ultraviolet, visible, and near infrared. *Journal of quantitative spectroscopy and radiative transfer*, 111(9):1289–1295, 2010.

Bo Galle, Mattias Johansson, Claudia Rivera, Yan Zhang, Manne Kihlman, Christoph Kern, Thomas Lehmann, Ulrich Platt, Santiago Arellano, and Silvana Hidalgo. Network for observation of volcanic and atmospheric change (novac)—a global network for volcanic gas monitoring: Network layout and instrument description. *Journal of Geophysical Research: Atmospheres*, 115(D5), 2010.

Minard L Hall, Claude Robin, Bernardo Beate, Patricia Mothes, and Michel Monzier. Tungurahua volcano, ecuador: structure, eruptive history and hazards. *Journal of Volcanology and Geothermal Research*, 91(1):1–21, 1999.

Silvana Hidalgo, Jean Battaglia, Santiago Arellano, Alexander Steele, Benjamin Bernard, Julie Bourquin, Bo Galle, Santiago Arrais, and Freddy Vásconez. So2 degassing at tungurahua volcano (ecuador) between 2007 and 2013: Transition from continuous to episodic activity. *Journal of Volcanology and Geothermal Research*, 298:1–14, 2015.

Christoph Kern. *Spectroscopic measurements of volcanic gas emissions in the ultraviolet wavelength region*. PhD thesis, 2009.

Stefan Kraus. *DOASIS: A framework design for DOAS*. Shaker, 2006.

Peter Lübcke. *Optical remote sensing measurements of bromine and sulphur emissions: Investigating their potential as tracers of volcanic activity*. PhD thesis, 2014.

Peter Lübcke, Nicole Bobrowski, S Arellano, Bo Galle, G Garzón, Leif Vogel, and U Platt. Bro/so 2 molar ratios from scanning doas measurements in the novac network. *Solid Earth*, 5(1):409, 2014.

D Perner and U Platt. Detection of nitrous acid in the atmosphere by differential optical absorption. *Geophysical Research Letters*, 6(12):917–920, 1979.

G Pinardi, MV Roozendael, and C Fayt. The influence of spectrometer temperature variability on the data retrieval of so2. *NOVAC second annual activity report, NOVAC consortium*, 44:48, 2007.

U Platt and N Bobrowski. Quantification of volcanic reactive halogen emissions. *Volcanism and Global Change, eds A. Schmidt, K. Fristad, L. Elkins-Tanton, Cambridge University Press, Cambridge, UK, ISBN*, 1466525386, 2015.

Ulrich Platt and Jochen Stutz. Differential absorption spectroscopy. *Differential Optical Absorption Spectroscopy*, pages 135–174, 2008.

Alan Robock. Volcanic eruptions and climate. *Reviews of Geophysics*, 38(2):191–219, 2000.

A Schmidt and A Robock. Volcanism, the atmosphere and climate through time. *Volcanism Glob. Environ. Chang*, pages 195–207, 2015.

Anja Schmidt, Kirsten Fristad, and Linda T Elkins-Tanton. Volcanism and global environmental change, 2015.

Hans-Ulrich Schmincke. *Vulkanismus.* Wissenschaftliche Buchgesellschaft, 3 edition, 2000.

S Solomon, RW Portmann, RR Garcia, W Randel, F Wu, R Nagatani, J Gleason, L Thomason, LR Poole, and MP McCormick. Ozone depletion at mid-latitudes: Coupling of volcanic aerosols and temperature variability to anthropogenic chlorine. *Geophysical research letters*, 25(11):1871–1874, 1998.

Susan Solomon, Arthur L Schmeltekopf, and Ryan W Sanders. On the interpretation of zenith sky absorption measurements. *Journal of Geophysical Research: Atmospheres*, 92(D7):8311–8319, 1987.

Thorvaldur Thordarson and Stephen Self. Atmospheric and environmental effects of the 1783–1784 laki eruption: A review and reassessment. *Journal of Geophysical Research: Atmospheres*, 108(D1), 2003.

T Wagner, A Apituley, S Beirle, S Dörner, U Friess, J Remmers, and R Shaiganfar. Cloud detection and classification based on max-doas observations. *Atmospheric Measurement Techniques*, 7(5):1289–1320, 2014.

Simon Warnach. Improvements of bro and so2 retrievals of novac data - tungurahua volcano as a case study. Master's thesis, 2015.